Transforming Growth Factor β1 Signaling via Interaction with Cell Surface Hyal-2 and Recruitment of WWOX/WOX1*ⓢ

Li-Jin Hsu[‡§¶1], Lori Schultz[¶], Qunying Hong[¶], Kris Van Moer[¶], John Heath[¶], Meng-Yen Li[‖], Feng-Jie Lai[**], Sing-Ru Lin[‡‡], Ming-Hui Lee[‡‡], Cheng-Peng Lo[‖], Yee-Shin Lin[‡§], Shur-Tzu Chen[‖2], and Nan-Shan Chang[§¶‡‡§§3]

From the [‡‡]Institute of Molecular Medicine, [‡]Departments of Microbiology and Immunology, [§]Center for Gene Regulation and Signal Transduction Research, [‖]Cell Biology and Anatomy, and [**]Dermatology, National Cheng Kung University Medical College, Tainan 70101, Taiwan, the [¶]Guthrie Research Institute, Laboratory of Molecular Immunology, Sayre, Pennsylvania 18840, and the [§§]Department of Neuroscience and Physiology, State University of New York Upstate Medical University, Syracuse, New York 13210

Transforming growth factor β (TGF-β) initiates multiple signal pathways and activates many downstream kinases. Here, we determined that TGF-β1 bound cell surface hyaluronidase Hyal-2 on microvilli in type II TGF-β receptor-deficient HCT116 cells, as determined by immunoelectron microscopy. This binding resulted in recruitment of proapoptotic WOX1 (also named WWOX or FOR) and formation of Hyal-2·WOX1 complexes for relocation to the nuclei. TGF-β1 strengthened the binding of the catalytic domain of Hyal-2 with the N-terminal Tyr-33-phosphorylated WW domain of WOX1, as determined by time lapse fluorescence resonance energy transfer analysis in live cells, co-immunoprecipitation, and yeast two-hybrid domain/domain mapping. In promoter activation assay, ectopic WOX1 or Hyal-2 alone increased the promoter activity driven by Smad. In combination, WOX1 and Hyal-2 dramatically enhanced the promoter activation (8–9-fold increases), which subsequently led to cell death (>95% of promoter-activated cells). TGF-β1 supports L929 fibroblast growth. In contrast, transiently overexpressed WOX1 and Hyal-2 sensitized L929 to TGF-β1-induced apoptosis. Together, TGF-β1 invokes a novel signaling by engaging cell surface Hyal-2 and recruiting WOX1 for regulating the activation of Smad-driven promoter, thereby controlling cell growth and death.

Transforming growth factor β (TGF-β)[4] plays a dual role in cell growth and tumorigenesis (1, 2). TGF-β inhibits mammary epithelial cell growth. In contrast, invasive cancer cells fre-quently overproduce TGF-β to promote growth and metastasis (1, 2). The underlying mechanism is largely unknown. TGF-β induces the development of metastatic phenotypes, i.e. stimulation of epithelial-mesenchymal transitions in cancerous mammary epithelial cells (1, 2). These cells are normally devoid of functional type II TGF-β receptor (TβRII), suggesting that TGF-β binds to an alternative receptor for signaling.

Hyaluronan is the major components of pericellular coat and plays a key role in affecting cell morphology, communication, and behavior (3–5). Up-regulation of hyaluronan and hyaluronidases Hyal-1, Hyal-2, and PH-20 is associated with cancer metastasis (3–5). Hyaluronidases counteract the activity of TGF-β1 (6–8). TGF-β1 suppresses the proliferation of normal epithelial cells, whereas PH-20 blocks the TGF-β1 effect (6). Hyal-1 and Hyal-2 enhance the cytotoxic function of TNF and block TGF-β1-mediated protection of murine L929 fibroblasts from TNF cytotoxicity (6–8).

Hyaluronidases PH-20, Hyal-1, and Hyal-2 induce the expression of tumor suppressor WW domain-containing oxidoreductase, known as WWOX, FOR or WOX1 (8–11). Human WWOX gene is located on a chromosomal fragile site 16q23 and encodes WWOX/FOR/WOX1 and isoforms (9, 10, 12–16). The full-length 46-kDa WOX1 possesses two N-terminal WW domains (containing conserved tryptophan residues), a nuclear localization sequence between the WW domains, and a C-terminal short chain alcohol dehydrogenase/reductase domain. Numerous exogenous stimuli, including sex steroid hormones, TNF, anisomycin, UV light, and apoptosis inducers, induce WOX1 activation via phosphorylation at Tyr-33 and nuclear translocation both in vivo and in vitro (9, 17–20).

Human and mouse WWOX/WOX1 appears to play a dual role in regulating cell survival and death (for review, see Ref. 10). Ectopic WOX1 exerts apoptosis in vitro (9, 17–22) and inhibits tumor growth in vivo (12, 22). Targeted deletion of murine Wwox gene to exons 2–4 induces spontaneous tumor formation in the lung and bone marrow (23). The whole body Wwox gene-ablated mice can only survive for approximately 1 month (23). Later on, murine Wwox gene was shown to be essential for postnatal survival and normal bone metabolism in mice (24)

and development of the reproductive system (25, 26). Indeed, several prior reports have clearly indicated that endogenous human and mouse WWOX/WOX1 is up-regulated at both gene and protein levels during embryonic development (27) and in the early stages of hyperplasia and cancerous progression of human breast and prostate (17, 28–31). Also, WWOX/WOX1 is up-regulated during normal skin keratinocyte differentiation as well as in the early stages of UVB-induced formation of squamous cell carcinoma in humans and mice (20). Again, these observations support the dual functional roles of WWOX/WOX1 in supporting cell survival, differentiation, and organogenesis and yet controlling cancer growth.

WOX1 binds numerous proteins in the stress signaling and apoptotic responses and factors in gene transcription (for reviews, see Refs. 10 and 32). In this study we investigated whether TGF-β1 signals via a pathway independently of TβRII and examined whether this signaling activates WOX1 for cell growth regulation. Here, we demonstrated a novel signaling involving the binding of TGF-β1 with membrane Hyal-2 and then recruiting WOX1. The resulting Hyal-2·WOX1 complexes relocate to the nuclei for controlling the activation of Smad-driven promoter, thereby regulating cell growth and death.

EXPERIMENTAL PROCEDURES

Cell Lines, Chemicals, Antibodies, and Polyclonal Antibody Production—Murine L929 fibroblasts and human TβRII-deficient colorectal HCT116 cells from American Type Culture Collections have been maintained in our laboratory (8, 9) and used in this study. Platelet-derived TGF-β1 was from R & D Systems, and recombinant TGF-β1 was from PeproTek. 4′,6-Diamidino-2-phenylindole was from Calbiochem.

We have generated polyclonal antibodies against 1) an N-terminal segment of WOX1 at the first WW domain (pan-specific for human, rat, and mouse) (17), 2) a WOX1 peptide with Tyr-33 phosphorylation at the first WW domain (pan-specific for human, rat, and mouse) (17), and 3) the unique C terminus of human WWOX/WOX1 (15). In addition, a synthetic peptide of murine Hyal-2, NH_2-CPDVEVARNDQLAWL-COOH (amino acids 227–241) was made (Genemed Synthesis). We generated polyclonal antibodies against this peptide in rabbits using an EZ antibody production and purification kit (Pierce), as described (9, 15, 17). The selected amino acid sequence of murine Hyal-2 is identical to that in human, pig, and rat. Also, this region is predicted to be a helical, surface-exposed segment, according to homology searching in the GenBank™ database for the three-dimensional structure of the lyco_hydro_56 domain (or catalytic domain) in hyaluronidase.

Additional specific antibodies used in Western blotting were against the following proteins: Smad4 (mouse and rabbit IgG from Zymed Laboratories Inc., Cell Signaling Technology, Upstate Biotechnology, and Santa Cruz Laboratories), Tyr-204-phosphorylated extracellular signal-regulated kinase (p-ERK, Santa Cruz Laboratories), CD44 (Chemicon); α-tubulin (Accurate Chemicals). WWOX IgG antibodies were gifts from Santa Cruz Laboratories and Abcam.

cDNA Expression Constructs, Transfection in Cell Lines, Fluorescence, Confocal Microscopy, and Immunoprecipitation—The following expression constructs were made; 1) murine EGFP-WOX1, full-length coding region of WOX1 cDNA tagged with enhanced green fluorescence protein (EGFP) in p-EGFP-C1 vector (Clontech) (9); 2) DN-WOX1, murine dominant-negative WOX1 tagged with EGFP (17); 3) EYFP-Hyal-2(GLYH), the catalytic domain of murine Hyal-2, tagged with enhanced yellow fluorescence protein (EYFP) in a p-EYFP-C1 vector (Clontech); 4) EGFP-Smad4, murine Smad4 tagged with EGFP (GenBank™ accession AY493561). In addition, we constructed an EGFP-tagged Hyal-2(EGF) construct in pEGFP-C1 vector (Clontech). This construct expresses the EGF domain (epidermal growth factor-like domain) of Hyal-2 (225 bp for the cDNA insert). We selected an antisense construct which allows expression of EGFP and a short stretch of antisense mRNA for Hyal-2, designated EGFP-Hyal-2(as). Primers for designing this construct were 1) forward 5′-TCGAATTCTATGTATTG-CAGTTGGACCAG, and 2) reverse 5′-CAGAATTCGAT-TATTGGCACTGCTCGCCACC. This antisense construct suppressed Hyal-2 protein expression in human, mouse, and rat. L929 or HCT116 cells were electroporated with the above constructs (200 volt, 50 ms; Square Wave BTX ECM830, Genetronics) (9, 17, 18), grown overnight, treated with TGF-β1, and then subjected to extraction and separation of cytosolic and nuclear fractions using the NE-PER Nuclear and Cytoplasmic Extraction reagent (Pierce). Albumin (0.5%) was included during electroporation to enhance electroporation efficiency (300–500% increase) and to limit electric shock-mediated cell death (18). Where indicated, these cell preparations were subjected to co-immunoprecipitation and Western blotting (9, 17, 18). In addition, cells were transfected with cDNA constructs using liposome-based FuGENE 6 (Roche Applied Science) or Genefector (VennNova). Both reagents were equally effective in gene transfection. Epifluorescence microscopy was carried out in some experiments using a Nikon Eclipse TE-2000U inverted microscope. Confocal microscopy was also performed to determine protein localization (Olympus FV1000).

TGF-β1 Cross-linking onto Cell Membrane and Immunoelectron Microscopy—HCT116 cells cultured on Petri dishes were washed 3 times with phosphate-buffered saline (PBS) and incubated with 0.25 μg/ml purified platelet TGF-β1 (in PBS containing 10 μg/ml bovine serum albumin; R&D Systems) on ice for 90 min. Disuccinimidyl suberate (Pierce), a chemical cross-linker, was prepared fresh and added to the cells (0.4 mM final concentration). The cells were kept on ice for 2 h, then rinsed with ice-cold phosphate-buffered saline and fixed with 4% paraformaldehyde in 0.1 M phosphate buffer (pH 7.2) on ice for 1 h. The samples were dehydrated in a graded series of ethanol and embedded in LR White resin (London Resin) in a 50 °C oven (33). Ultrathin sections (70–80 nm; ultramicrotome, from Reichert-Jung) were prepared and incubated with selected combinations of two of the following antibodies: rabbit polyclonal anti-WOX1, anti-Hyal-2, goat polyclonal anti-human WWOX (Santa Cruz Biotechnologies), or mouse monoclonal anti-TGF-β (R&D systems). These sections were then stained with anti-rabbit IgG (conjugated
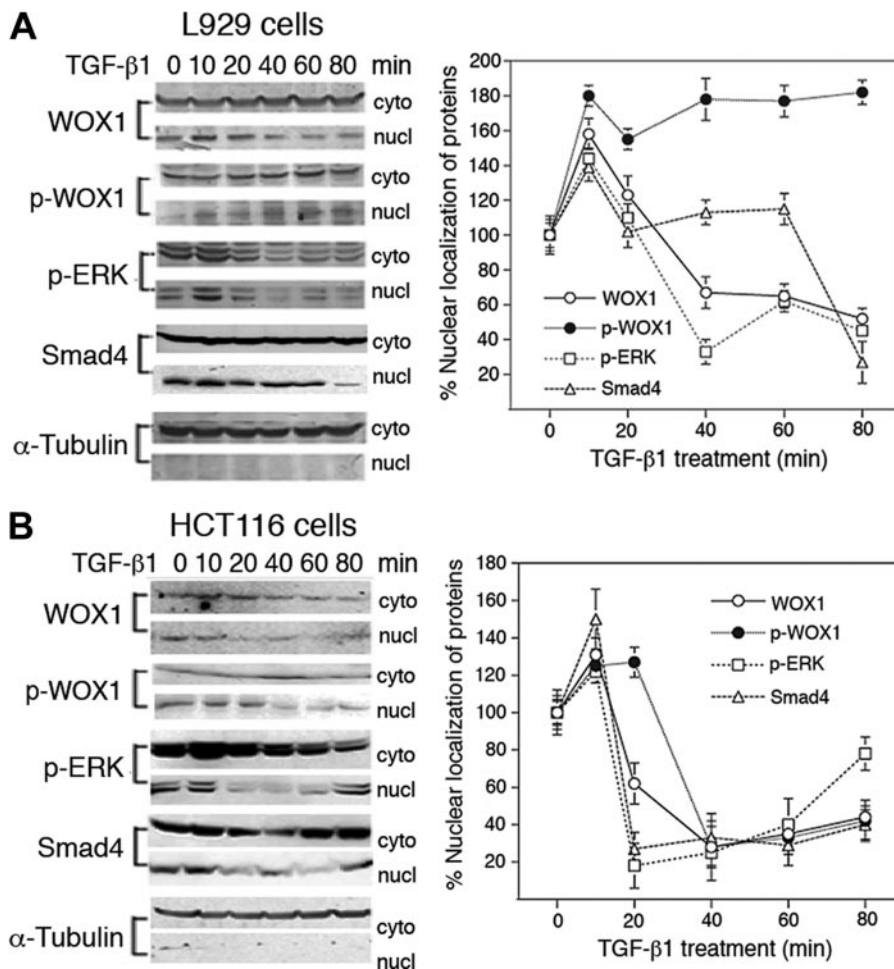
FIGURE 1. **TGF-β1 rapidly induces accumulation of WOX1 in the nuclei.** *A*, exposure of L929 cells to TGF-β1 (5 ng/ml) rapidly induced accumulation of WOX1, p-WOX1, Smad4, and p-ERK in the nuclei in 10–20 min. The bands in Western blots were quantified (mean ± S.D., *n* = 5). The nuclear level of each indicated protein is regarded as 100% at time 0. *p-WOX1*, Tyr-33-phosphorylated WOX1. *p-ERK*, Tyr-204-phosphorylated ERK. *B*, under similar conditions, HCT116 cells were treated with TGF-β1 (5 ng/ml) and shown to have relocation of the above-mentioned proteins to the nuclei (mean ± S.D., *n* = 3). *Cyto*, cytosol; *nucl*, nucleus.

length WOX1, the N-terminal first WW domain, or a Y33R mutant of the WW domain (in a pSos vector; Stratagene) and the Hyal-2 construct for membrane-anchoring (in a pMyr vector; Stratagene). Colony growth and selection were then performed (9, 17, 18). For positive controls, WOX1/p53 physical association and MafB self-interaction were carried out. Empty pSos/pMyr vectors were regarded as negative controls, which yielded no yeast colonies (9, 17, 18).

Förster (Fluorescence) Resonance Energy Transfer (FRET)—The full-length murine WOX1 and the catalytic domain of murine Hyal-2 were constructed in-frame with ECFP and EYFP expression vectors (Clontech), respectively. L929 and HCT116 cells were transfected with both constructs by liposome-based Genefector (VennNova) and cultured for 24–48 h. FRET analysis was performed using an inverted fluorescence microscope (Nikon Eclipse TE-2000U). Cells were stimulated with an excitation wavelength 440 nm. FRET signals were detected at an emission wavelength 535 nm (see Fig. 6A for the schematic). ECFP and EYFP were used as donor and acceptor fluorescent molecules, respectively. The FRET images were corrected for background fluorescence from an area free of cells and spectral bleed-through. The spectrally corrected FRET concentration (FRETc) was calculated by Youvan's equation (using a software program Image-Pro 6.1, Media Cybernetics): FRETc = [fret − bk(fret)] − cf(don) × [don − bk(don)] − cf(acc) × [acc − bk(acc)], where fret = fret image, bk = background, cf = correction factor, don = donor image, and acc = acceptor image. The equation normalizes the FRET signals to the expression levels of the fluorescent proteins.

Promoter Activation Assay—An assay kit for the promoter function driven by Smad was from SABiosciences. HCT116 and L929 cells were transfected with a promoter construct using green fluorescent protein as a reporter by electroporation (200 volt and 50 ms; using a BTX ECM830 electroporator from Genetronics) or using liposome-based FuGENE 6 (Roche Applied Science) or Genefector (VennNova). Also, expression constructs for WOX1, Hyal-2(GLYH), DN-WOX1, and/or Smad4 were included in the mixtures for electroporation. The cells were cultured for 24 h. Promoter activation was examined under fluorescence microscopy. Both positive and negative controls from the assay kit were also tested in each experiment.

with 20-nm gold particle) and anti-goat or anti-mouse IgG (conjugated with 10-nm gold particle) antibodies (BB International Ltd). Specimens were counterstained with saturated aqueous uranyl acetate and lead citrate at room temperature and examined under a transmission electron microscopy (JEOL JEM-1200EX, Japan) at 100 kV.
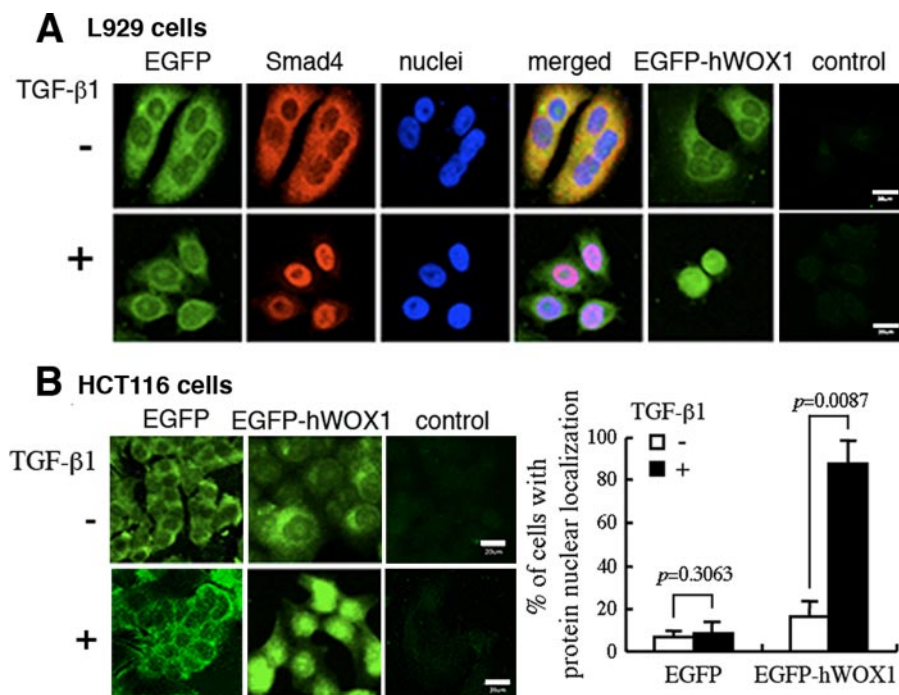
Yeast Two-hybrid Analysis—Ras rescue-based CytoTrap yeast two-hybrid analysis (Stratagene) was performed to map the domain/domain interaction between Hyal-2 and WOX1, as described (9, 17, 18). Briefly, bait protein was tagged with Sos, and target protein was tagged with a membrane-anchoring signal sequence (Stratagene). Binding of the cytosolic Sos-tagged bait protein to the cell membrane-anchored target activates the Sos/Ras/Raf/MEK/ERK signal pathway, thereby allowing the growth of mutant yeast *cdc25H* at 37 °C under a synthetic defined galactose media (−Ura,−Leu) in agarose plates. That is, the occurrence of positive protein/protein binding and subsequent activation of the Sos/Ras/Raf/MEK/ERK signaling promotes yeast cells to grow at 37 °C, whereas at room temperature (22 °C) all yeast cells grow in the selective medium (9, 17, 18). Yeast cells were transfected with a bait construct (*e.g.* the full-

FIGURE 2. **TGF-β1-induced WOX1 relocation to the nuclei as determined by confocal microscopy.** *A*, L929 cells were transfected with EGFP or human WOX1/WWOX (EGFP-hWOX1) using FuGENE 6 followed by culturing for 24 h and then stimulating with TGF-β1 for 4 h. The prolonged treatment was to optimize protein migration, as the protein was tagged with EGFP. By confocal microscopy, EGFP-hWOX1 and endogenous Smad4 were shown to accumulate in the nuclei (>95% nuclear localization for both proteins; ~150 cells from 3 experiments). In EGFP-expressing cells, TGF-β1 caused nuclear accumulation of endogenous Smad4 (>97%) but not EGFP (~1%). *Control*, non-transfected cells. *B*, similarly, HCT116 cells were transiently overexpressed with EGFP or EGFP-hWOX1, and exposure of these cells to TGF-β1 (5 ng/ml) for 4 h resulted in accumulation of EGFP-hWOX1, but not EGFP, in the nuclei (mean ± S.D.; ~150 cells were counted from three experiments). For Student's *t* tests, controls *versus* cells treated with TGF-β1. *Scale bar* = 20 μm (for *A* and *B*). *Controls*, non-transfected cells (see also supplemental Figs. S1 and S2).

RESULTS

TGF-β1 Induces WOX1 Nuclear Relocation in a TβRII-independent Manner—We examined whether TGF-β1 stimulates relocation of WOX1 to the nuclei in murine L929 fibroblasts. These cells are responsive to TGF-β1-induced proliferation (6–8). Also, TGF-β1 protects L929 cells from the cytotoxic effect of tumor necrosis factor (6–8). L929 fibroblasts were cultured overnight in RPMI medium, supplemented with 10% heat-inactivated fetal bovine serum. In time-course experiments, stimulation of murine L929 fibroblasts with purified human platelet TGF-β1 resulted in a rapid nuclear relocation of WOX1 and its Tyr-33-phosphorylated form (or activated WOX1; p-WOX1) in 10–20 min, as determined by Western blotting (Fig. 1*A*). Fetal bovine serum was included in the assay. Similar results were observed using recombinant human TGF-β1 (data not shown). A similar kinetics for the nuclear relocation of Tyr-204-phosphorylated extracellular signal-regulated kinase (p-ERK) and Smad4 was also observed (Fig. 1*A*). Fetal bovine serum in the cell culture constitutively sustains low levels of phosphorylation in WOX1 and ERK (6, 8).

For comparison, we utilized the TβRII-negative human colorectal HCT116 cell line (34, 35). TGF-β1 does not induce phosphorylation of Smad2/3 for forming complexes with Smad4 and subsequent translocation to the nuclei in these cells. We examined whether TGF-β1 induces WOX1 relocation to the nuclei in a TβRII-independent manner. Exposure of HCT116

cells to TGF-β1 also resulted in nuclear translocation of WOX1, p-WOX1, Smad4, and p-ERK in a time-related manner, as shown in Western blotting (Fig. 1*B*). However, TGF-β1 was less effective in exerting the effect in HCT116 cells than in L929 cells.

In similar experiments, L929 cells were transfected with EGFP or human WOX1/WWOX (EGFP-hWOX1) by liposome-based FuGENE 6. After 24 h of culture, cells were stimulated with platelet TGF-β1 for 4 h. Significant accumulation of EGFP-hWOX1 and endogenous Smad4 in the nuclei was shown (>95% nuclear localization for both proteins; ~150 cells counted from 3 experiments), as determined by confocal microscopy (Fig. 2*A*). In EGFP-expressing cells, TGF-β1 significantly caused relocation of endogenous Smad4 to the nuclei (>97%) (Fig. 2*A*). However, TGF-β1 did not induce EGFP alone relocation to the nuclei (~1%; Fig. 2*A*). To prevent retardation of protein migration due to the EGFP tag, L929 cells were treated with TGF-β1 for a prolonged period up to 4 h.

In parallel, HCT116 cells were transfected with EGFP or EGFP-hWOX1 by liposome-based FuGENE 6 followed by culturing for 24 h and then exposure to TGF-β1 for 4 h. Significant accumulation of EGFP-hWOX1, but not EGFP, in the nuclei was observed (Fig. 2*B*).

In additional experiments, L929 cells were treated with TGF-β1 for the indicated times up to 2 h. The extent of relocation of endogenous WOX1 and Smad4 in the nuclei was quantified (see *micrographs* and *bar graphs* in supplemental Fig. S1). TGF-β1 effectively induced accumulation of endogenous WOX1 and Smad4 in the nuclei in L929 cells in a time-related manner (~70% in 1 h).

Under similar conditions, HCT116 cells were treated with TGF-β1 for 1 h. The data showed that TGF-β1 induced nuclear accumulation of WOX1 and isoform WOX2 in a dose-related manner, as determined by Western blotting (supplemental Fig. S2*A*). Similarly, TGF-β1 induced accumulation of WOX1 in the nuclei, as determined by immunofluorescence microscopy (Fig. 2*B*). Compared with L929 cells, TGF-β1 was less effective in inducing nuclear relocation of endogenous WOX1 in HCT116 cells (~30% in 1 h; supplemental Fig. S2*B*). The function of WOX2 has never been documented in the literature, whereas its expression is significantly down-regulated in patients with Alzheimer disease (15). Taken together, our observations show that TGF-β1-induced WOX1 relocation to
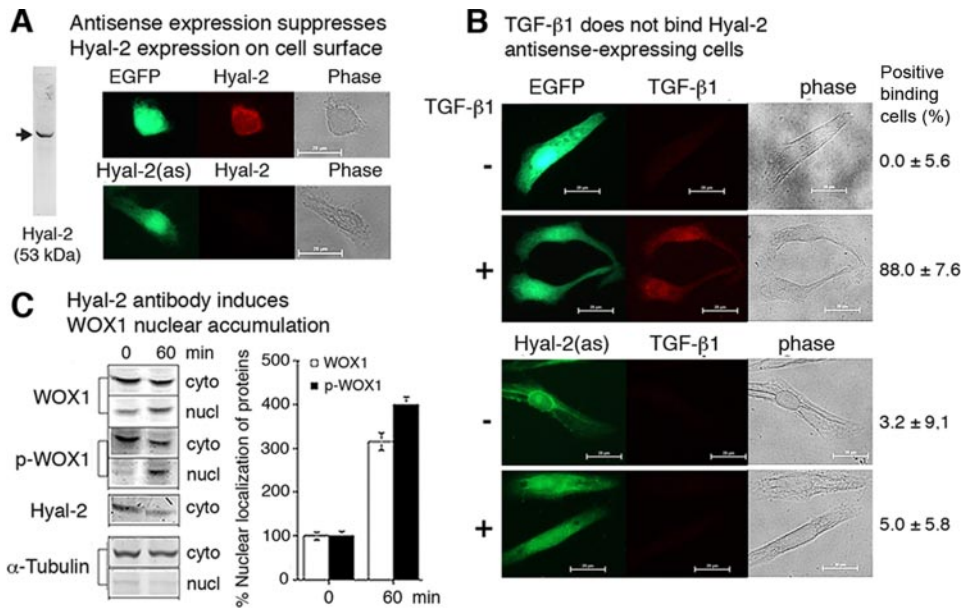
FIGURE 3. **TGF-β1 binds to cell surface Hyal-2.** *A*, antibody was produced against a synthetic Hyal-2 peptide and shown to interact with a 53-kDa Hyal-2 in L929 cells, as determined by Western blotting. L929 cells were electroporated with an EGFP-tagged Hyal-2-antisense construct, EGFP-Hyal-2(as) (see "Experimental Procedures"), and cultured for 48 h. The Hyal-2 antisense-expressing cells exhibited green fluorescence and had a significantly reduced expression of cell surface Hyal-2 (*red* fluorescence for Hyal-2 using antibody stain; 5.7 ± 2.2% positive in total cells, *n* = 3) compared with EGFP-expressing cells (92 ± 7.2% positive, *n* = 3) and non-transfected cells (93 ± 4.8% positive, *n* = 3). *B*, TGF-β1 did not bind to the surface of Hyal-2 antisense-expressing L929 cells, as compared with EGFP-expressing cells or non-transfected cells (>85% binding). That is, the percentage of positive binding cells showed the TGF-β1 signal (*red*) above the background control cells. *C*, stimulation of L929 cells with anti-Hyal-2 antiserum (1/500 final dilution) for 1 h induced significant accumulation of WOX1 and p-WOX1 in the nuclei compared with the levels at time 0 (mean ± S.D., *n* = 3; *p* = 0.013 for WOX1 and *p* = 0.0025 for p-WOX1, Student's *t* tests; see the *bar graph*). The background WOX1 phosphorylation was due to fetal bovine serum in the cell culture. Non-immune serum had no apparent effect in inducing WOX1 nuclear relocation (data not shown).

L929 cell surface was blocked (supplemental Fig. S3), suggesting that TGF-β1 binds Hyal-2 to this surface-exposed segment. In appropriate control experiments, we tested several peptides with similar compositions. None of these was found to block the binding of TGF-β1 onto cell surface (data not shown).

To further examine the specific role of Hyal-2 in signaling, cell surface Hyal-2 was cross-linked with our produced antibodies followed by determining relocation of WOX1 to the nuclei. Stimulation of L929 cells with diluted Hyal-2 antiserum resulted in accumulation of WOX1 (and p-WOX1) in the nuclei (Fig. 3*C*), whereas non-immune control serum had no effect (data not shown). These observations suggest that our produced Hyal-2 antibody acts as a specific agonist in inducing WOX1 nuclear relocation or activation.

TGF-β1 Binds to Membrane Hyal-2 on Microvilli as Determined by Immunoelectron Microscopy— Next, we examined the morphological aspect on how TGF-β1 interacts with Hyal-2 by immunoelectron

the nuclei is independent of the signaling starting from the binding of TGF-β1 with cell surface TβRII.

TGF-β1 Binds Cell Surface Hyal-2 and Induces WOX1 Accumulation in the Nuclei— We investigated whether TGF-β1 activates WOX1 via signaling through cell surface hyaluronidase Hyal-2 but not TβRII. We have shown that WOX1 binds Hyal-2 as determined in yeast two-hybrid cDNA library screening (9, 17). In addition, we have shown that Hyal-2 enhances the apoptotic function of WOX1 (8).

Hyal-2 is present in the lysosome (36) and on the cell surface as a glycosylphosphatidylinositol-anchored form (37). We synthesized a Hyal-2 peptide for polyclonal antibody production in rabbits. This peptide sequence corresponds to a surface-exposed segment in the lyco_hydro_56 or catalytic domain of hyaluronidase (5). The produced antibody recognized a predicted 53-kDa Hyal-2 protein in L929 cells (Fig. 3*A*). Cell surface expression of Hyal-2 was shown in a high percentage of L929 cell population transfected with EGFP or buffer only (Fig. 3*A*). When L929 cells were transfected with the Hyal-2 antisense construct (tagged with EGFP), expression of cell surface Hyal-2 was significantly reduced (Fig. 3*A*). Binding of TGF-β1 to the surface of Hyal-2 antisense-expressing cells was significantly reduced (<10% binding, Fig. 3*B*). In EGFP-transfected or non-transfected controls, binding of TGF-β1 to the surface of these cells was not affected (~85% binding; Fig. 3*B*).

When purified platelet TGF-β1 was pre-mixed with the synthetic Hyal-2 peptide for 30 min at 4 °C, binding of TGF-β1 to

microscopy. TβRII-deficient HCT116 cells were used in these experiments, so that there was no binding of TGF-β1 to the cell surface TβRII. Purified platelet TGF-β1 was shown to interact with Hyal-2 on cell surface microvilli. There were ~1–5 TGF-β1·Hyal-2 particles per microvillus as determined from 10 sections (Fig. 4, *A* and *B*, and supplemental Fig. S4). Briefly, HCT116 cells were exposed to purified TGF-β1 at 4 °C for 90 min. TGF-β1 was then covalently cross-linked onto cell membrane by disuccinimidyl suberate. In negative control cells, albumin was cross-linked onto cell membrane. Essentially, little or no nonspecific binding was observed in control cells (supplemental Fig. S4).

Hyal-2 is involved in the catabolism of hyaluronan (5). The Hyal-2·hyaluronan complex is internalized by endocytic vesicles and then fused with lysosomes. Hyaluronan is then degraded. Similarly, stimulation of cells with TGF-β1 at 37 °C resulted in complex formation of TGF-β1·Hyal-2 on the cell membrane followed by internalization via endocytic vesicles (endosomes) and fusion with lysosomes (Fig. 4*B*). In agreement with another report (36), Hyal-2 alone is present in the lysosome (Fig. 4*B*; see *box c*).

TGF-β1 Increases the Complex Formation of Hyal-2 and WOX1— In unstimulated HCT116 cells, a portion of endogenous WOX1 was physically associated with membrane Hyal-2 on microvilli, as determined by immunoelectron microscopy (Fig. 5*A*). WOX1 alone also was present in a close proximity to the cell membrane area (Fig. 5*A*; see the *star*). The
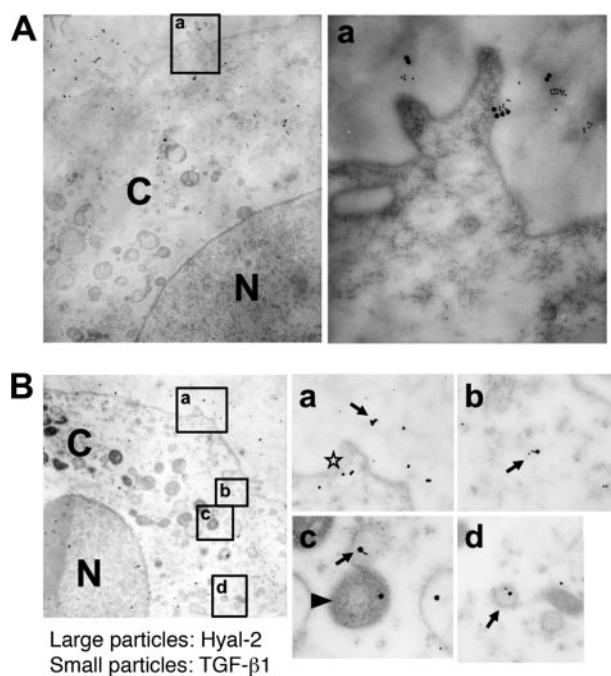
FIGURE 4. **TGF-β1 binds to cell surface Hyal-2 on microvilli followed by internalization via endosomes.** *A*, TβRII-negative HCT116 cells were exposed to 250 ng/ml TGF-β1 (in phosphate-buffered saline containing 10 μg/ml bovine serum albumin) on ice for 90 min followed by processing disuccinimidyl suberate cross-linking and immunoelectron microscopy. Exogenous TGF-β1 bound membrane Hyal-2 mainly on microvilli (colocalization of large and small immunogold particles; magnification ×6000). There were ~1–5 TGF-β1·Hyal-2 particles per microvillus as determined from 10 sections. *Hyal-2*, labeled with specific anti-Hyal-2 antibody and 20 nm anti-rabbit immunogold particles (see large particles); *TGF-β1*, labeled with specific anti-TGF-β1 IgG and 10 nm anti-mouse immunogold particles (see small particles). An *enlarged image* at the *right panel* is from a *boxed area* in the *left panel* (magnification ×50,000). Similar results and negative controls are shown in supplemental Fig. S4. *B*, similarly, HCT116 cells were stimulated with TGF-β1 (5 ng/ml) for 30 min. Immunoelectron microscopy showed the presence of TGF-β1·Hyal-2 complexes on the microvillus (*arrow*; see the *enlarged image* from *box a*), in the internalized endocytic vesicles (*box b*; *arrow*), and endosomes (see *boxes c* and *d*; *arrows*). Hyal-2 alone is shown in the endocytic vesicle (*star*; *box a*). Fusion of an endosome with a lysosome (*arrowhead*) is shown in *box c*. Magnification: *left*, ×10,000; *a–d*, ×50,000. *C*, cytoplasm; *N*, nucleus.

WOX1·Hyal-2 complexes were found in the cytosol (Fig. 5*A*). TGF-β1 increased the complex formation of WOX1·Hyal-2 and its nuclear translocation (Figs. 5*B* and supplemental Fig. S5). In most cases HCT116 cells have large nuclei and relatively thin cytoplasmic areas; however, the cytoplasmic areas are increased when the cells fully spread out on a plastic surface (supplemental Fig. S2). Accordingly, there were higher numbers of WOX1·Hyal-2 complexes in the nucleus than in the cytoplasm, as averaged from random measurements in 2.5 μm² areas (Fig. 5*C*). Nuclear accumulation of these complexes either on nuclear envelopes or in nuclei was increased upon exposure to TGF-β1 with time (Fig. 5*C*). Again, in negative controls, these immunogold particles did not non-specifically interact with each other. TGF-β1 alone did not bind WOX1 (data not shown).

Hyal-2 and CD44 are co-receptors for hyaluronan (5). By immunoelectron microscopy, we determined that CD44 did not bind TGF-β1 or WOX1 at the membrane and cytosolic areas in HCT116 cells, treated with or without TGF-β1 (data not shown).
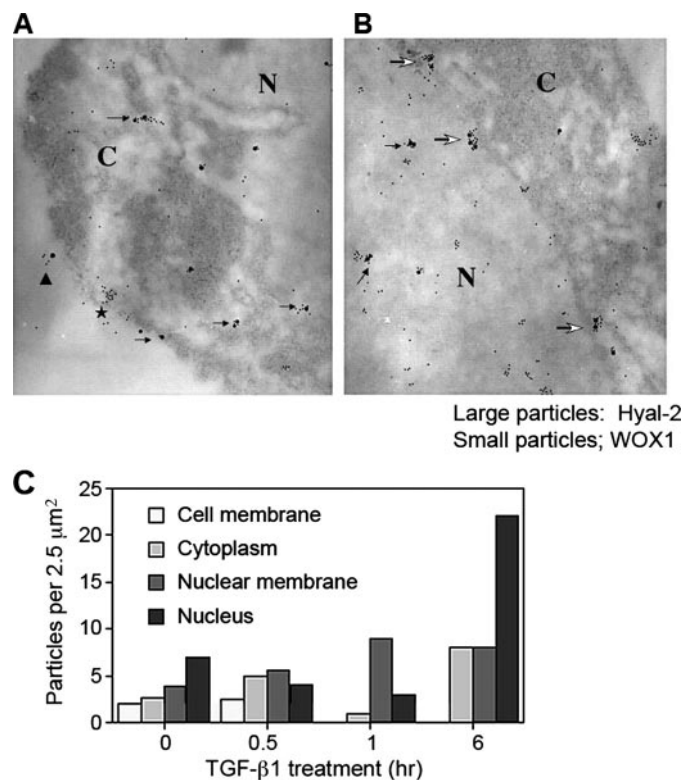

FIGURE 5. **TGF-β1 increases complex formation of Hyal-2 and WOX1 in HCT116 cells analyzed by immunoelectron microscopy.** *A*, HCT116 cells were cultured in the presence of 10% fetal bovine serum overnight. A portion of endogenous WOX1 is physically associated with membrane Hyal-2 on microvilli (*dark triangle*). WOX1 is present in close proximity to the cell membrane (*star*) as well as in other areas in the cytoplasm. The presence of WOX1·Hyal-2 complexes is found in the cytoplasm and nucleus (*arrows*). *B*, stimulation of cells with TGF-β1 (5 ng/ml) for 30 min resulted in an increased complex formation of WOX1 and Hyal-2 along with nuclear translocation, which was shown on the nuclear membrane (see the *open arrows*) and inside the nucleus (*arrows*). In negative controls, these immunogold particles did not non-specifically interact with each other (data not shown). Hyal-2 was labeled with specific anti-Hyal-2 antibody and 20-nm anti-rabbit immunogold particles (see large particles); WOX1 was labeled with specific anti-WWOX IgG and 10-nm anti-goat immunogold particles (see small particles). *C*, cytoplasm; *N*, nucleus. Magnification: ×40,000. *C*, HCT116 cells were treated with TGF-β1 (5 ng/ml) for the indicated times. The numbers of WOX1·Hyal-2 particles were measured at subcellular locations, including cell membrane, cytoplasm, nuclear membrane, and nuclei (data shown as averages from 2–3 measurements in 2.5 μm² areas). Note that HCT116 cells possess large nuclei but relatively thin cytoplasmic areas.

TGF-β1 Enhances the Binding of WOX1 with Hyal-2 (FRET Analysis), and the Protein Complexes Sensitize L929 Fibroblasts to TGF-β1-induced Apoptosis—Next, we examined the kinetics of Hyal-2·WOX1 complex formation. L929 cells were co-transfected with the full-length murine WOX1 (tagged with ECFP) and the catalytic domain of murine Hyal-2 (tagged with EYFP) (5, 8), followed by culturing for 24–48 h. The cells were treated with TGF-β1, and pictures were taken for every 10 min for cyan fluorescence protein, yellow fluorescence protein, and FRET signals. We determined that TGF-β1 rapidly increased the binding of WOX1 with Hyal-2 in 20 min (10–30% increase; see FRETc in *red*), followed by reduction 1 h after (30–80% reduction; Fig. 6). The specific FRET signals were calculated to eliminate background fluorescence and spectral bleed-through. In negative controls, ECFP did not bind FYFP and produced no signals (data not shown).
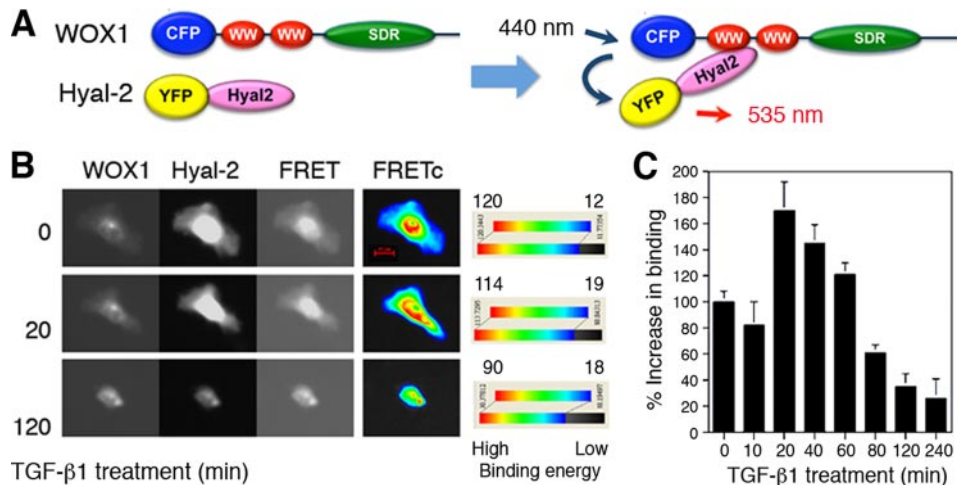
FIGURE 6. **Hyal-2·WOX1 complexes sensitize L929 cells to TGF-β1-mediated apoptosis as analyzed by time-lapse microscopy and FRET.** *A*, a schematic diagram for the binding of WOX1 with Hyal-2 by FRET analysis (see "Experimental Procedures") is shown. The full-length murine WOX1 was tagged with ECFP, and the catalytic domain of murine Hyal-2(GLYH) was tagged with EYFP. *B*, L929 cells were transfected with these constructs and then cultured for 48 h followed by treating with TGF-β1 (5 ng/ml) for live cell FRET analysis in time-lapse microscopy. TGF-β1 rapidly increased the binding of WOX1 with Hyal-2 in 20 min, as evidenced by an increased binding energy (shown in *red*). The specific FRET signals were calculated as FRET concentration (*FRETc*) to eliminate background fluorescence and spectral bleed-through. A color scale is shown for the strength of binding. *Scale bar* = 10 μm. *C*, percent pixel changes for the strongest binding areas (*red*) are quantified and tabulated (mean ± S.D.; *n* = 5). In negative controls, ECFP did not bind FYFP and produced no signals (data not shown). The cell underwent apoptosis, as evidenced by reduction in cell sizes with time, membrane blebbing (see also supplemental Fig. S6), and formation of apoptotic bodies (at 80 min). *CFP*, cyan fluorescent protein; *YFP*, yellow fluorescent protein; *SDR*, short-chain alcohol dehydrogenase/reductase.
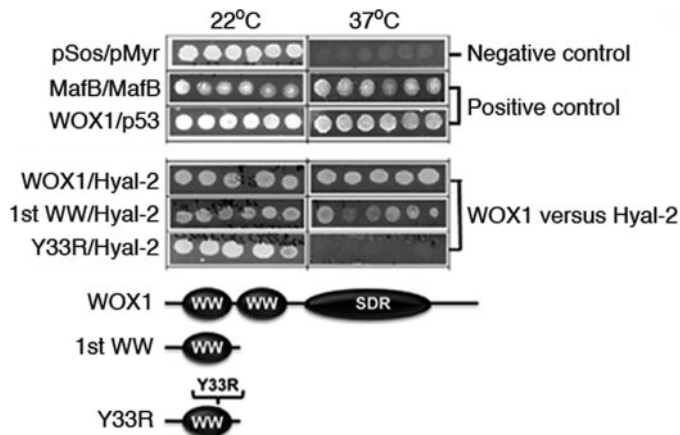
FIGURE 7. **Hyal-2 binds to the N-terminal first WW domain of WOX1.** Cyto-Trap or Ras rescue-based yeast two-hybrid analysis for protein/protein interaction in the cytoplasm was performed (see "Experimental Procedures") (9, 17, 18, 38–40). In positive controls, binding of cytosolic WOX1 with membrane-bound p53 resulted in activation of the Sos/Ras/Raf/MEK/ERK signaling, thus allowing yeast cells to grow at 37 °C in selective galactose medium in agarose plate (see the representative colonies). Similar results were shown for the MafB self-interaction. In negative controls, no yeast growth at 37 °C was observed for the empty pSos/pMyr vectors. Live yeast cells grow normally at room temperature (22 °C), bypassing the Sos/Ras/Raf/MEK/ERK signaling. The N-terminal first WW domain of Wox1 (*1stWW*) bound Hyal-2. Alteration of Tyr-33 to Arg-33 in the first WW domain (Y33R) abolished its interaction with Hyal-2.

Notably, when L929 cells were overexpressed with WOX1 and Hyal-2, these cells became sensitized to TGF-β1-induced apoptosis, including reduction in cell sizes (60% in 1 h and 80% in 4 h), membrane blebbing, and formation of apoptotic bodies (Figs. 6 and supplemental Fig. S6). The observations are in stark contrast to the growth-promoting effect of TGF-β1 on L929 cells (8). In comparison, when L929 cells were overexpressed

with ECFP-Hyal-2 and EYFP-Hyal-2 (both catalytic domains), these cells were resistant to TGF-β1-induced apoptosis (supplemental Fig. S6).

Hyal-2 Binds WOX1 at the Tyr-33-phosphorylated First WW Domain—We utilized the CytoTrap yeast two-hybrid system to determine how WOX1 physically binds Hyal-2 (9, 17, 18, 38–40). Hyal-2 was anchored onto the cell membrane as a binding target, and various WOX1 constructs were tagged with Sos protein and expressed in the cytoplasm as protein bait (Fig. 7). Yeast cells were co-transfected with the expression constructs of the Hyal-2 and an indicated WOX1. When the expressed Sos-WOX1 protein physically interacted with the membrane-bound Hyal-2, yeast cells grew at 37 °C in a selective galactose medium in agarose plates because of activation of the Sos/Ras/Raf/MEK/ERK pathway (see representative colonies in Fig. 7). Without binding, no cell growth occurred (Fig. 7). The yeast cells were alive as they grew at room temperature (22 °C) (Fig. 7). Hyal-2 physically interacted with WOX1 via its N-terminal first WW domain (Fig. 7). No binding interaction was observed using a phosphorylation mutant, Wox1ww(Y33R), indicating an essential role of Tyr-33 phosphorylation in the binding. As a negative control, no binding interactions were observed when empty pSos and pMyr vectors were used. In positive controls, WOX1/p53 binding and MafB self-interaction were shown (Fig. 7).

To verify the above observations, HCT116 cells were cotransfected with a set of each indicated ECFP-WOX1 and EYFP-Hyal-2 constructs using liposome-based FuGENE 6 or Genefector, followed by culturing for 48 h. FRET analysis revealed that the N-terminal first WW domain of WOX1 physically interacted with the catalytic domain of Hyal-2 (Hyal-2(GLYH); 210 ± 55 and 310 ± 48% increases in binding for the full-length WOX1 and WW domain with Hyal-2, respectively; *n* = 10; compared with non-binding ECFP/EYFP controls). The binding occurred strongly in the nuclei (data not shown). The C-terminal short chain alcohol dehydrogenase/reductase domain did not interact with Hyal-2 (0 ± 4% increase; *n* = 10). Hyal-2 did not undergo self binding (51 ± 4% increase; *n* = 10). The FRET experiments were also carried out using L929 cells, which yielded similar results (data not shown).

We further verified the WOX1·Hyal-2 complex formation by co-immunoprecipitation. Stimulation of L929 cells with TGF-β1 increased the formation of WOX1·Hyal-2 complex, as precipitated using anti-WOX1 antibody (Fig. 8A). Similar results were observed with HCT116 cells stimulated with TGF-β1 (Fig. 8B). We have developed a dominant-negative
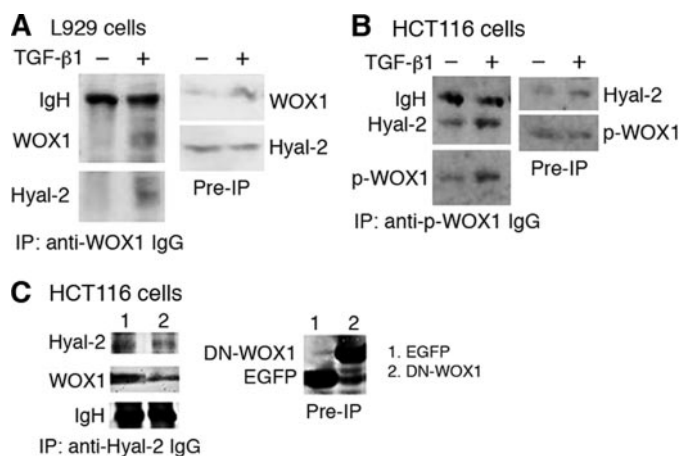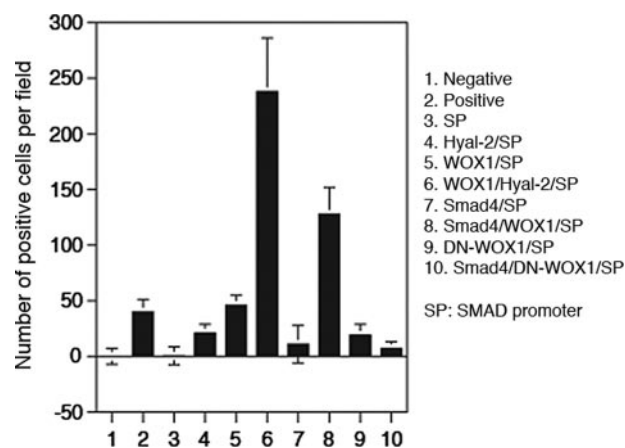
FIGURE 8. **TGF-β1 increases the complex formation of Hyal-2 and WOX1, as determined by co-immunoprecipitation.** *A*, L929 cells were stimulated with TGF-β1 (5 ng/ml) for 30 min, which resulted in increased formation of WOX1·Hyal-2 complex, as determined by co-immunoprecipitation with antibody against WOX1. *Pre-IP*, $^1/_{20}$ amounts of protein samples for immunoprecipitation were loaded onto SDS-PAGE (~30 µg). *B*, similarly, HCT116 cells were stimulated with TGF-β1 (5 ng/ml) for 30 min, followed by immunoprecipitation with anti-p-WOX1 IgG. TGF-β1 increased the binding of Hyal-2 with WOX1. *C*, HCT116 cells were transiently overexpressed with a dominant-negative WOX1 (*DN-WOX1*; tagged with EGFP) or EGFP alone. DN-WOX1 inhibited the WOX1·Hyal-2 complex formation (reduction by 32 ± 4%, *n* = 3).

FIGURE 9. **WOX1 and Hyal-2 dramatically enhance promoter activation driven by Smad proteins for subsequent cell death.** HCT116 cells were transfected with a Smad-driven promoter (*SP*) construct (using green fluorescent protein as reporter) in the presence or absence of WOX1, Hyal-2(GLYH), Smad4, and/or DN-WOX1 constructs. Both negative and positive control vectors were also used. After culturing for 24 h, the extent of promoter activation was measured as the number of cells with green fluorescence (10 fields counted per cell preparation on cover slide; 3 experiments; mean ± S.D.). The extent of cell death was 98 and 95% in promoter-activated cells transfected with WOX1·Hyal-2 and WOX1·Smad4, respectively (measured from 4′,6-diamidino-2-phenylindole staining). Compared with positive control cells, these condensed, apoptotic cells exhibited smaller green fluorescent dots. Approximately 2–20% death was observed in cells transfected with WOX1, Hyal-2, Smad4, DN-WOX1, or the promoter alone. No cell death was shown in both the positive and negative control cells.

WOX1 (DN-WOX1) and shown its inhibition of stress-induced WOX1 phosphorylation at Tyr-33 (17, 18). Ectopic expression of DN-WOX1 reduced the WOX1·Hyal-2 complex formation (reduction by 32 ± 4%, *n* = 3; Fig. 8*C*), suggesting that phosphorylation of WOX1 at Tyr-33 is essential for interacting with Hyal-2.

WOX1 and Hyal-2 Synergistically Enhance the Promoter Activation Driven by Smad Proteins for Subsequent Cell Death— Next, we determined whether WOX1 and Hyal-2 affect the transcriptional activation of promoter driven by Smad proteins. HCT116 cells were transfected with a Smad-driven promoter construct (using green fluorescent protein as a reporter) in the presence or absence of the WOX1 and/or Hyal-2(GLYH) constructs (Fig. 9). WOX1 or Hyal-2 alone limitedly increased the transcriptional activation of the Smad promoter (Fig. 9). Together, both proteins dramatically enhanced the transcriptional activation of the Smad promoter in a synergistic manner (increase by 8–9-fold; Fig. 9). Ectopic Smad4 alone was not sufficient to induce the transcriptional activation, whereas in combination, both WOX1 and Smad4 significantly enhanced the promoter activation. Again, DN-WOX1 is a potent inhibitor of WOX1 phosphorylation at Tyr-33 (or activation) as well as a suppressor of p53-meidated cell death (17, 18). No promoter activation occurred when both DN-WOX1 and Smad4 were co-transfected in the cells (Fig. 9).

Notably, there was 98 and 95% death in the promoter-activated cells transfected with WOX1·Hyal-2 and WOX1·Smad4, respectively (determined by 4′,6-diamidino-2-phenylindole staining). Much less death was shown for cells transfected with WOX1, Hyal-2, Smad4, DN-WOX1, or the promoter alone (~2–20% death). No cell death was shown in both the positive and negative controls. The experiment was also carried out in L929 cells, which showed similar results (data not shown).

DISCUSSION

In this study we have shown for the first time that cell surface hyaluronidase Hyal-2 is a cognate receptor for TGF-β1. TGF-β1 binds Hyal-2 on the microvilli of the plasma membrane. This binding allows internalization of TGF-β1·Hyal-2 complexes via endosomes and then fusion of lysosomes with the internalized endosomes. Whether this event leads to degradation of TGF-β1 in the lysosomes is unknown.

We determined the TGF-β1·Hyal-2·WOX1 signaling by immunoelectron microscopy, time-lapse FRET analysis in live cells, yeast two-hybrid analysis, and co-immunoprecipitation. The sequential signaling event involves the following. 1) TGF-β1 binds plasma membrane Hyal-2 to a surface-exposed segment in the catalytic domain, 2) the binding rapidly promotes the complex formation of WOX1 and Hyal-2, and 3) the WOX1·Hyal-2 complexes relocate to the nuclei for enhancing promoter activation driven by Smad proteins (Fig. 10*A*).

Alternatively, the membrane TGF-β1·Hyal-2 complexes are internalized via endocytic vesicles. Hyal-2 is then released to the cytoplasm followed by interacting with cytosolic WOX1 and the resulting Hyal-2·WOX1 complexes relocating to the nuclei (Fig. 10*B*).

Finally, from the promoter activation assays, we determined that WOX1 and Smad4, when in combination, dramatically activated the promoter function, suggesting that WOX1 physically interacts with Smad4 and that Smad4 is associated with the Hyal-2·p-WOX1 complexes. That is, binding of TGF-β1 to the cell membrane Hyal-2 results in recruitment of p-WOX1 and Smad4. Then, the Hyal-2·p-WOX1·Smad4 complexes relocate to the nuclei (Fig. 10*C*). The protein complexes bind the Smad promoter via Smad4, thus effectively leading to promoter
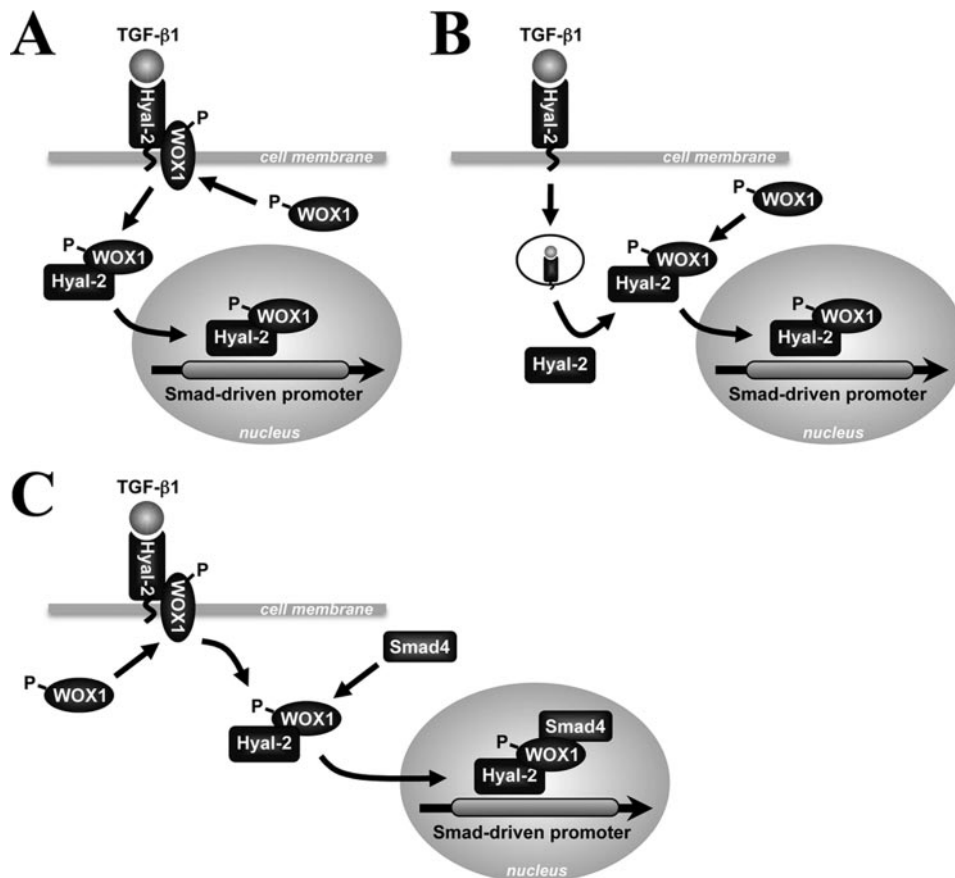
FIGURE 10. **TGF-β1·Hyal-2·WOX1 signaling.** Three likely signaling paths are as follows. *A*, TGF-β1 binds membrane Hyal-2 that subsequently recruits cytosolic Tyr-33-phosphorylated WOX1 (*p-WOX1*) to the membrane. The resulting Hyal-2·p-WOX1 complexes translocate to the nuclei for enhancing the promoter function driven by endogenous Smad proteins. Overly activated Smad promoter induces cell death. *B*, alternatively, the TGF-β1·Hyal-2 complexes are internalized via endocytic vesicles followed by releasing of Hyal-2 to the cytoplasm for interacting with the cytosolic p-WOX1 and the p-WOX1·Hyal-2 complexes relocating to the nuclei. *C*, an additional scenario is that Smad4 is recruited to the p-WOX1·Hyal-2 complexes followed by relocating to the nuclei. This event is supported by our finding that when in combination, both WOX1 and Smad4 dramatically increased the Smad promoter activation.

inositol linkage for membrane anchorage (37). It is not clear whether all the newly synthesized Hyal-2 effectively translocates to the cytoplasmic membrane, or it may reside on the membranous structures of subcellular organelles. We have shown that induction of the mitochondrial pathway of apoptosis by staurosporine induces relocation of Hyal-2 to the mitochondria (8). Under stress conditions, WOX1 translocates to the mitochondria both *in vitro* and *in vivo* (9, 19, 42, 43) and causes cytochrome *c* release from the mitochondria (44). Thus, Hyal-2 and WOX1 are likely to co-translocate, as complexes, to the mitochondria during apoptosis.

WW domains are involved in protein-protein interactions and signal transduction (45). WW domain-containing proteins may transmit signals to membrane cytoskeleton (46). Human WWOX is known to interact with ezrin, a component of the ezrin-radixin-moesin signaling from extracellular matrix hyaluronan to the membrane/cytoskeletal system (47). Protein kinase A phosphorylates ezrin, and that phosphorylated ezrin is essential for anchoring WWOX onto the apical area in gastric parietal cells (47). One of our recently identified WWOX/WOX1-binding proteins is tumor suppressor merlin/NF-2 (type II neurofibromatosis).[5] Merlin/NF-2 provides a signal link from hyaluronan·Hyal-2 to cytoskeletal ezrin-radixin-moesin proteins (48). TGF-β1 is expected to activate this signal pathway to exert growth suppression from direct interaction with Hyal-2. Additionally, human WWOX binds membrane ErbB4 receptor, thereby reducing nuclear translocation of the cleaved intracellular domain of ErbB4 and inhibiting its transactivation function mediated through Yes-associated protein (49, 50).

Like other members of hyaluronidases, Hyal-2 possesses a catalytic domain. This domain has several helical segments consisting of a catalytic residue and four positioning residues for substrates (5). Our produced antibody, targeting amino acids 227–241, does not recognize the catalytic residue Glu-135 in Hyal-2 (5). Interestingly, the antibody mimics the TGF-β1 function in stimulating WOX1 accumulation in the nuclei. The synthetic peptide for antibody production blocks TGF-β1 binding to the surface of TβRII-positive L929 cells, suggesting

activation. Smad4 participates in promoter activation (41), and thus, WOX1 can be considered as a co-factor for Smad4. Transiently overexpressed Hyal-2 and/or WOX1 are capable of activating the Smad promoter in HCT116 cells, raising the possibility that Hyal-2 or WOX1 binds the promoter DNA and controls its activation.

It appears that there is a very close functional relationship between Hyal-2 and TβRII. When TβRII-positive L929 cells were transiently overexpressed with the Hyal-2 antisense RNA, binding of TGF-β1 to the cell surface was abolished. Also, pretreatment of cells with antibody against Hyal-2 followed by subsequent challenge with TGF-β1 abolished WOX1 nuclear relocation (data not shown). The observations suggest that Hyal-2 may physically interact with TβRII on the cell membrane. Or, their binding is enhanced upon challenging the cells with TGF-β1 or cross-linking Hyal-2 with specific antibodies. These likely scenarios have yet to be tested.

In agreement with previous observations (36), we show the presence of Hyal-2 alone in the lysosomes, as determined by immunoelectron microscopy. Whether the lysosomal Hyal-2 relocates directly from the cell surface is unknown and requires further investigation. Hyal-2 possesses a glycosylphosphatidyl-

---

[5] N.-S. Chang, M. H. Lee, S. R. Lin, and C. I. Sze, unpublished information.

that Hyal-2 can act alone as a receptor and is involved in anchoring TGF-β1 onto cell surface.

Hyal-2 is also a known co-receptor with CD44 for hyaluronan. CD44 does not participate in the TGF-β1-induced nuclear translocation of WOX1. By co-immunoprecipitation and immunoelectron microscopy, we determined that TGF-β1 does not interact with CD44 nor does WOX1 interact with CD44 (data not shown). Nonetheless, CD44 may colocalize with TGF-β receptors, which allows hyaluronan to affect TGF-β signaling in both supportive and suppressive manners in different types of cells (51, 52).

WOX1 interacts with several transcription factors such as p53 (9, 17, 18), p73 (53), AP2γ (54), ErbB2 (55), and ErbB4 (49, 50). Among these, p53 is known to participate in TGF-β signaling at various points in the pathway by interacting with Smad proteins (56, 57). Thus, p53 may participate in the transcriptional regulation by interacting with WOX1·Hyal-2·Smad4. Whether p53 enhances or blocks the function of WOX1·Hyal-2 complexes in supporting cell growth or enhancing death remains to be determined.

Upon stimulation with TGF-β1, WOX1 may translocate to the cell surface and bind Hyal-2 via its N-terminal WW domains, as evidenced by both immunofluorescence staining and immunoelectron microscopy. This binding depends upon Tyr-33 phosphorylation in the WW domains. Tyr-33 phosphorylation of WOX1 probably occurs in the cytosol before translocation to the cell surface. Src is known to phosphorylate WOX1 at Tyr-33 (10, 32). The presence of WOX1·Hyal-2 complexes on the nuclear membrane or envelope is intriguing. We have determined the presence of a mitochondria-targeting sequence in the C-terminal short chain alcohol dehydrogenase/reductase domain of WOX1 (9). We propose that the membrane insertion of WOX1 is mediated through this mitochondria-targeting sequence.

Finally, we have shown that sex steroid hormones (*e.g.* estrogen and androgen) up-regulate and activate WWOX/WOX1, isoform WOX2, p53, and ERK in COS7 fibroblasts, primary lung epithelial cells, and androgen receptor-negative prostate DU145 cells but not in estrogen receptor-positive breast MCF7 cells (19). Prolonged activation of WOX1 may render apoptosis in COS7 cells. Failure of sex steroid hormones in stimulating the activation of WOX1 and WOX2 in benign breast cancer cells (19) suggests that Hyal-2 retains WOX1 and WOX2 on the cell membrane and blocks its tumor suppressor function. Invasive breast cancer cells are frequently deficient in the wild type WOX1 (19, 29). Overexpressed WOX2 effectively induces apoptosis as that of WOX1,[5] whereas the physiological function of WOX2 is largely unknown. Whether WOX2 and other isoforms act as dominant negatives in blocking the function of wild type WWOX/WOX1 is unknown. Also, whether these proteins bind Hyal-2 and block the TGF-β1·Hyal-2 signaling, thereby enhancing cancer growth, remains to be established.

REFERENCES

1. Muraoka-Cook, R. S., Dumont, N., and Arteaga, C. L. (2005) *Clin. Cancer Res.* **11,** 937S–943S
2. Bachman, K. E., and Park, B. H. (2005) *Curr. Opin. Oncol.* **17,** 49–54
3. Udabage, L., Brownlee, G. R., Nilsson, S. K., and Brown, T. J. (2005) *Exp. Cell Res.* **310,** 205–217
4. Cattaruzza, S., and Perris, R. (2005) *Matrix Biol.* **24,** 400–417
5. Stern, R., and Jedrzejas, M. J. (2006) *Chem. Rev.* **106,** 818–839
6. Chang, N. S. (1997) *Am. J. Physiol.* **273,** C1987–1994
7. Chang, N. S. (1998) *Int. J. Mol. Med.* **2,** 653–659
8. Chang, N. S. (2002) *BMC Cell Biol.* **3,** 8
9. Chang, N. S., Pratt, N., Heath, J., Schultz, L., Sleve, D., Carey, G. B., and Zevotek, N. (2001) *J. Biol. Chem.* **276,** 3361–3370
10. Chang, N. S., Hsu, L. J., Lin, Y. S., Lai, F. J., and Sheu, H. M. (2007) *Trends Mol. Med.* **13,** 12–22
11. Lokeshwar, V. B., Cerwinka, W. H., Isoyama, T., and Lokeshwar, B. L. (2005) *Cancer Res.* **65,** 7782–7789
12. Bednarek, A. K., Keck-Waggoner, C. L., Daniel, R. L., Laflin, K. J., Bergsagel, P. L., Kiguchi, K., Brenner, A. J., and Aldaz, C. M. (2001) *Cancer Res.* **61,** 8068–8073
13. Ried, K., Finnis, M., Hobson, L., Mangelsdorf, M., Dayan, S., Nancarrow, J. K., Woollatt, E., Kremmidiotis, G., Gardner, A., Venter, D., Baker, E., and Richards, R. I. (2000) *Hum. Mol. Genet.* **9,** 1651–1663
14. Smith, D. I., McAvoy, S., Zhu, Y., and Perez, D. S. (2007) *Semin. Cancer Biol.* **17,** 31–41
15. Sze, C. I., Su, M., Pugazhenthi, S., Jambal, P., Hsu, L. J., Heath, J., Schultz, L., and Chang, N. S. (2004) *J. Biol. Chem.* **279,** 30498–30506
16. Mahajan, N. P., Whang, Y. E., Mohler, J. L., and Earp, H. S. (2005) *Cancer Res.* **65,** 10514–10523
17. Chang, N. S., Doherty, J., and Ensign, A. (2003) *J. Biol. Chem.* **278,** 9195–9202
18. Chang, N. S., Doherty, J., Ensign, A., Schultz, L., Hsu, L. J., and Hong, Q. (2005) *J. Biol. Chem.* **280,** 43100–43108
19. Chang, N. S., Schultz, L., Hsu, L. J., Lewis, J., Su, M., and Sze, C. I. (2005) *Oncogene* **24,** 714–723
20. Lai, F. J., Cheng, C. L., Chen, S. T., Wu, C. H., Hsu, L. J., Lee, J. Y., Chao, S. C., Sheen, M. C., Shen, C. L., Chang, N. S., and Sheu, H. M. (2005) *Clin. Cancer Res.* **11,** 5769–5777
21. Qin, H. R., Iliopoulos, D., Semba, S., Fabbri, M., Druck, T., Volinia, S., Croce, C. M., Morrison, C. D., Klein, R. D., and Huebner, K. (2006) *Cancer Res.* **66,** 6477–6481
22. Fabbri, M., Iliopoulos, D., Trapasso, F., Aqeilan, R. I., Cimmino, A., Zanesi, N., Yendamuri, S., Han, S. Y., Amadori, D., Huebner, K., and Croce, C. M. (2005) *Proc. Natl. Acad. Sci. U. S. A.* **102,** 15611–15616
23. Aqeilan, R. I., Trapasso, F., Hussain, S., Costinean, S., Marshall, D., Pekarsky, Y., Hagan, J. P., Zanesi, N., Kaou, M., Stein, G. S., Lian, J. B., and Croce, C. M. (2007) *Proc. Natl. Acad. Sci. U. S. A.* **104,** 3949–3954
24. Aqeilan, R. I., Hassan, M. Q., de Bruin, A., Hagan, J. P., Volinia, S., Palumbo, T., Hussain, S., Lee, S. H., Gaur, T., Stein, G. S., Lian, J. B., and Croce, C. M. (2008) *J. Biol. Chem.* **283,** 21629–21639
25. Ludes-Meyers, J. H., Kil, H., Nuñez, M. I., Conti, C. J., Parker-Thornburg, J., Bedford, M. T., and Aldaz, C. M. (2007) *Genes Chromosomes Cancer* **46,** 1129–1136
26. Aqeilan, R. I., Hagan, J. P., de Bruin, A., Rawahneh, M., Salah, Z., Gaudio, E., Siddiqui, H., Volinia, S., Alder, H., Lian, J. B., Stein, G. S., and Croce, C. M. (2009) *Endocrinology* **150,** 1530–1535
27. Chen, S. T., Chuang, J. I., Wang, J. P., Tsai, M. S., Li, H., and Chang, N. S. (2004) *Neuroscience* **124,** 831–839
28. Watanabe, A., Hippo, Y., Taniguchi, H., Iwanari, H., Yashiro, M., Hirakawa, K., Kodama, T., and Aburatani, H. (2003) *Cancer Res.* **63,** 8629–8633
29. Guler, G., Uner, A., Guler, N., Han, S. Y., Iliopoulos, D., Hauck, W. W., McCue, P., and Huebner, K. (2004) *Cancer* **100,** 1605–1614
30. Płuciennik, E., Kusińska, R., Potemski, P., Kubiak, R., Kordek, R., and Bednarek, A. K. (2006) *Eur. J. Surg. Oncol.* **32,** 153–157
31. Driouch, K., Prydz, H., Monese, R., Johansen, H., Lidereau, R., and Frengen, E. (2002) *Oncogene* **21,** 1832–1840
32. Aqeilan, R. I., and Croce, C. M. (2007) *J. Cell Physiol.* **212,** 307–310
33. Chuang, J. I., Chen, S. T., Chang, Y. H., and Jen, L. S. (2001) *J. Chem. Neuroanat.* **21,** 215–223
34. Jiang, W., Tillekeratne, M. P. M., Brattain, M. G., and Banerji, S. S. (1997) *Biochemistry* **36,** 14786–14793
35. Wang, J., Sergina, N., Ko, T. C., Gong, J., and Brattain, M. G. (2004) *J. Biol. Chem.* **279,** 40237–40244

36. Lepperdinger, G., Strobl, B., and Kreil, G. (1998) *J. Biol. Chem.* **273,** 22466–22470

37. Rai, S. K., Duh, F. M., Vigdorovich, V., Danilkovitch-Miagkova, A., Lerman, M. I., and Miller, A. D. (2001) *Proc. Natl. Acad. Sci. U. S. A.* **98,** 4443–4448

38. Hong, Q., Hsu, L. J., Schultz, L., Pratt, N., Mattison, J., and Chang, N. S. (2007) *BMC Mol. Biol.* **8,** 50

39. Chang, N. S. (2002) *J. Biol. Chem.* **277,** 10323–10331

40. Schultz, L., Khera, S., Sleve, D., Heath, J., and Chang, N. S. (2004) *DNA Cell Biol.* **23,** 67–74

41. Schmierer, B., and Hill, C. S. (2007) *Nat. Rev. Mol. Cell Biol.* **8,** 970–982

42. Chen, S. T., Chuang, J. I., Cheng, C. L., Hsu, L. J., and Chang, N. S. (2005) *Neuroscience* **130,** 397–407

43. Lo, C. P., Hsu, L. J., Li, M. Y., Hsu, S. Y., Chuang, J. I., Tsai, M. S., Lin, S. R., Chang, N. S., and Chen, S. T. (2008) *Eur. J. Neurosci.* **27,** 1634–1646

44. Hsu, L. J., Hong, Q., Schultz, L., Kuo, E., Lin, S. R., Lee, M. H., Lin, Y. S., and Chang, N. S. (2008) *Cell. Signal.* **20,** 1303–1312

45. Sudol, M., Chen, H. I., Bougeret, C., Einbond, A., and Bork, P. (1995) *FEBS Lett.* **369,** 67–71

46. Ilsley, J. L., Sudol, M., and Winder, S. J. (2002) *Cell. Signal.* **14,** 183–189

47. Jin, C., Ge, L., Ding, X., Chen, Y., Zhu, H., Ward, T., Wu, F., Cao, X., Wang, Q., and Yao, X. (2006) *Biochem. Biophys. Res. Commun.* **341,** 784–791

48. Okada, T., You, L., and Giancotti, F. G. (2007) *Trends Cell Biol.* **17,** 222–229

49. Aqeilan, R. I., Donati, V., Gaudio, E., Nicoloso, M. S., Sundvall, M., Korhonen, A., Lundin, J., Isola, J., Sudol, M., Joensuu, H., Croce, C. M., and Elenius, K. (2007) *Cancer Res.* **67,** 9330–9336

50. Aqeilan, R. I., Donati, V., Palamarchuk, A., Trapasso, F., Kaou, M., Pekarsky, Y., Sudol, M., and Croce, C. M. (2005) *Cancer Res.* **65,** 6764–6772

51. Bourguignon, L. Y., Singleton, P. A., Zhu, H., and Zhou, B. (2002) *J. Biol. Chem.* **277,** 39703–39712

52. Ito, T., Williams, J. D., Fraser, D., and Phillips, A. O. (2004) *Am. J. Pathol.* **164,** 1979–1988

53. Aqeilan, R. I., Pekarsky, Y., Herrero, J. J., Palamarchuk, A., Letofsky, J., Druck, T., Trapasso, F., Han, S. Y., Melino, G., Huebner, K., and Croce, C. M. (2004) *Proc. Natl. Acad. Sci. U. S. A.* **101,** 4401–4406

54. Aqeilan, R. I., Palamarchuk, A., Weigel, R. J., Herrero, J. J., Pekarsky, Y., and Croce, C. M. (2004) *Cancer Res.* **64,** 8256–8261

55. Qin, H. R., Iliopoulos, D., Nakamura, T., Costinean, S., Volinia, S., Druck, T., Sun, J., Okumura, H., and Huebner, K. (2007) *Mol. Cancer Res.* **5,** 957–965

56. Atfi, A., and Baron, R. (2008) *Sci. Signal.* **1,** pe33

57. Cordenonsi, M., Dupont, S., Maretto, S., Insinga, A., Imbriano, C., and Piccolo, S. (2003) *Cell* **113,** 301–314